Direct Collapse Supermassive Black Holes from Relic Particle Decay

Yifan Lu[1,*], Zachary S. C. Picker,[1,†] and Alexander Kusenko[1,2,‡]

[1]*Department of Physics and Astronomy, University of California Los Angeles, Los Angeles, California 90095-1547, USA*
[2]*Kavli Institute for the Physics and Mathematics of the Universe (WPI), The University of Tokyo Institutes for Advanced Study, The University of Tokyo, Chiba 277-8583, Japan*

We investigate the formation of high-redshift supermassive black holes (SMBHs) via the direct collapse of baryonic clouds, where the unwanted formation of molecular hydrogen is successfully suppressed by a Lyman-Werner (LW) photon background from relic particle decay. We improve on existing studies by dynamically simulating the collapse, accounting for the adiabatic contraction of the DM halo, as well as the *in situ* production of the LW photons within the cloud which reduce the impact of the cloud's shielding. We find a viable parameter space where the decay of either some of the dark matter or all of a subdominant decaying species successfully allows direct collapse of the cloud to a SMBH.

The formation of the supermassive black holes (SMBHs) which reside in active galactic nuclei (AGN) and distant quasars remains an open question [1–6], dramatically reignited by recent observations from the James Webb Space Telescope (JWST) [7] of high-redshift ($z \gtrsim 6$) active galactic nuclei [8–15]. In light of these discoveries, many proposals were made for the creation of these SMBHs, including from the death of Pop III stars [16–18], grav-othermal collapse of self-interacting dark matter halos [19–23], primordial black holes (PBHs) [24–37], and, finally, the direct collapse of gas clouds [1,6,38–48].

The latter "direct collapse" scenario succeeds if the gas collapses and forms one central black hole instead of fragmenting into disjoint smaller clouds. Cooling by molecular hydrogen (H_2) leads to this fragmentation [49,50] and therefore suppression of H_2 formation ensures the direct collapse [38–40,51–55]. This can be achieved either by direct dissociation [1,40–47,56–63] or by excess heating [6,48]. The formation of a supermassive black hole from this successful collapse, including the resolution of the angular momentum transport problem [1,64–79] and the formation and collapse of a supermassive star as an intermediate phase [73–79], has been studied extensively and is now well established.

It is natural to ask if either the excess heating or the required Lyman-Werner (LW) background for dissociation could be provided by the decay of a relatively light particle. This particle could either make up all of the dark matter (DM), in which case the decay rate must be small on the cosmological timescales, or it could be a subdominant

component of DM that decays entirely around the epoch of reionization. Notably, the abundance of SMBH produced via this mechanism can be adequately explained by the expected mass function of halos at early times [46].

In this Letter, we extend the formalism developed in Ref. [46], and show that there is a viable parameter space where relic decaying particles [80–86] could lead to direct collapse. Specifically, these could be axionlike particles (ALPs) [87–98] which comprise all of the DM, or it could be a generic particle decaying at high redshifts, for example, one of the many particles in a string axiverse [95]. We model the direct collapse by a self-consistent dynamical evolution model of the DM halo's adiabatic contraction and chemical evolution, which is highly coupled and features significant feedback. On top of this, we reexamine the effect of the baryons' self-shielding of the LW radiation, arguing that the *in situ* production of radiation should significantly (if not completely) suppress the effect of shielding. When this is taken into account, we find that this mechanism of direct collapse is indeed viable for fractions of decaying dark matter well below observational constraints [99–101].

Cloud collapse—The direct collapse of a baryon cloud is a complex dynamical process and hydrodynamic simulation is often needed to study the evolution of the system. However, it has been demonstrated that a simpler approach, the one-zone model [53], can capture the essential ingredients of the direct collapse and offer accurate estimations of key quantities such as the photodissociation rate k_{H_2} and photodetachment rate k_{H^-} [60,102,103]. In the traditional one-zone model, the baryon cloud collapses inside a virialized DM halo that remains constant after the initial top-hat collapse phase. This approximation is acceptable for tracking the temperature and chemical evolution of the cloud only when the LW radiation is treated as a *constant* background.

*Contact author: yifanlu@g.ucla.edu
†Contact author: zpicker@physics.ucla.edu
‡Contact author: kusenko@ucla.edu

The density evolution of the cloud must be supplemented with Boltzmann equations which track H_2 and other chemical components during the collapse. In particular, the dominant H_2 formation channel requires an intermediate product H^-:

$$H + e^- \rightarrow H^- + \gamma, \quad (1)$$

$$H + H^- \rightarrow H_2 + e^-. \quad (2)$$
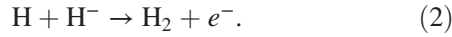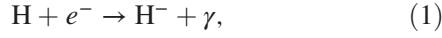
The destruction of H_2 can be accomplished by either directly dissociating H_2 with LW photons (photodissociation), or suppression of the formation of H^- via photons of energy $\gtrsim 0.76$ eV (photodetachment) [104]. The success of direct collapse to SMBHs critically depends on the specific radiation intensity $J(E)$ in these energy ranges and, consequently, the reaction rates k_{H_2} and k_{H^-}.

In our model, the LW radiation is directly coupled to the cloud evolution since it comes from the DM halo itself, and it is no longer a constant background. To calculate the DM density during this phase, we adopt a modified one-zone model which is supplemented with an explicit modeling of the adiabatic contraction of the DM halo [48,105–110], where the DM halo contracts in response to the collapse of the baryonic cloud. We follow the notations and conventions used in Ref. [48] with the following exceptions: the photodetachment rate k_γ in Ref. [48] only comes from the cosmic microwave background (CMB) spectrum, whereas we replace it here with the rate $k_\gamma + k_{H^-}$. Consequently, this leads to the modification of the equilibrium H^- fraction:

$$x_{H^-} = \frac{k_9 x_H x_e n}{k_\gamma + k_{H^-} + (k_{13} + k_{19}) x_e n + (k_{10} + k_{20}) x_H n}. \quad (3)$$

In addition, we now must include the photodissociation rate from the LW radiation in the x_{H_2} equation:

$$\frac{dx_{H_2}}{dt} = k_{10} x_H x_{H^-} n - k_{15} x_H x_{H_2} n - k_{18} x_e x_{H_2} n - k_{H_2} x_{H_2}. \quad (4)$$

Particle decay—Let us consider two particle models: a slowly decaying DM particle (as in the ALP scenario), and a subdominant component of an extended dark sector which is more rapidly decaying at the epoch of interest. We will refer to the former as DM and the latter as particle X. The decay of the particle produces a time dependent radiation-specific intensity $J(E, z)$ (in units of J/cm^2/s/Hz/sr) in the gas cloud given by [46]

$$J(\vec{r}, E, z) = \frac{E}{4\pi} \int dV' \frac{dn_\gamma}{dEdt} (\vec{r'}, E, z) \frac{1}{(\vec{r'} - \vec{r})^2}. \quad (5)$$

This expresssion—although completely general—is computationally intensive since keeping track of the spatial dependence is highly impractical. In addition, we take the

DM halo and the baryon cloud to have uniform density in the one-zone model, so the reaction rates are also position independent. This motivates us to simplify the specific intensity by using a spherically symmetric halo and computing its value at the center:

$$J(E, z) = E \int dr' \frac{dn_\gamma}{dEdt} (r', E, z). \quad (6)$$

The one-zone differential injection rate, $dn_\gamma/dEdt$ is given by

$$\frac{dn_\gamma}{dEdt} (E, z) = \frac{f_X(z) \Gamma \overline{\rho}_{DM}}{m} \frac{dN}{dE} (E), \quad (7)$$

where f_X is the time-dependent energy fraction of X compared to the total DM (if our decaying particle is all of the DM, $f_X = 1$). In Eq. (7), we assume that photons are the only decay products and neglect other possibilities, such as neutrinos or dark radiation (if they were to be included, our results will simply scale with the branching ratio of the photon decay channel). Our one-zone approximation contrasts with the "critical curve" approach where $J(E, z)$ is calculated using a nontrivial halo density profile [46]. We will map our results to the critical curve plot for comparison.

The shape of the decay spectrum dN/dE depends on the number of decay products. For ALPs, it is well motivated to consider two-body decay:

$$E \frac{dN}{dE} = 2\delta \left(1 - \frac{2E}{m_X} \right). \quad (8)$$

Following Ref. [46], we also consider three-body decay with an energy-independent decay amplitude, modeled with the so-called "parabola spectrum":

$$E \frac{dN}{dE} = 6 \left[\frac{E}{m_X} - \left(\frac{E}{m_X} \right)^2 \right] \Theta \left(1 - \frac{E}{m_X} \right). \quad (9)$$

The chemical rates k_{H^-} and k_{H_2} can be computed using the specific intensity [102]:

$$k_{H^-}(z) = \int_{0.76 \text{ eV}}^{13.6 \text{ eV}} 4\pi \sigma_{H^-}(E) \frac{J(E, z)}{E} \frac{dE}{h},$$

$$k_{H_2}(z) \approx 1.39 \times 10^{-12} \text{ s}^{-1} \frac{J_{LW}(z)}{J_{21}}, \quad (10)$$

where we take the cross section σ_{H^-} given in Ref. [104] and $J_{21} = 10^{-21}$ ergs^{-1} Hz^{-1} cm^{-2} sr^{-1}. Here, J_{LW} is calculated by taking the average of $J(E, z)$ in the LW band due to the complex structure of the rotational-vibrational states of H_2.

We note regarding Eq. (10) that previous studies used either constant spectra or black body spectra with

temperatures 10^4 or 10^5 K [53,60–63]. While the three-body decay spectrum is still continuous and will not deviate far from the approximations in Eq. (10), two-body decay could potentially alter the dissociation rate, as photons from the decay are monochromatic, and the absorption spectrum of H_2 is discrete. This does not present a problem: the typical timescale for the collapse is $\Delta z \sim 1$, during which the photon energy is redshifted by ~ 0.5 eV if the halos collapse around $z = 20$. The redshift and the thermal Doppler broadening allow the radiation to cover the fine spaced rotational-vibrational energy levels [111]. The spectral energy distribution (SED) in our model is different from the black body SED widely studied in the literature. This fact, together with the dynamic nature of the radiation intensity, makes a direct comparison with the critical intensity found in previous simulations impractical.

Shielding—The rate given in Eq. (10) is valid only in the optically thin regime, and additional treatment is necessary when the column density of H_2 reaches the critical value of 10^{14} cm^{-2}. Beyond this density, the H_2 becomes optically thick to LW radiation and the gas is self-shielding, reducing the dissociation rate by a fraction $f_{\rm shield}(N_{H_2}, T)$. We adopt a shielding fraction as in Ref. [112] that takes into account thermal broadening effects. The full density-dependent dissociation rate is then

$$k_{H_2}(N_{H_2}, T) = k_{H_2} f_{\rm shield}(N_{H_2}, T). \tag{11}$$

In practice, computing the H_2 column density is intractable in cosmological simulations. In Ref. [113], it was shown that the column density is best approximated by

$$N_{H_2} = \frac{1}{4} n_{H_2} \lambda_{\rm Jeans}, \tag{12}$$

where $\lambda_{\rm Jeans}$ is the Jeans length. We will use this equation to calculate the column density and the shield fraction.

The magnitude of $f_{\rm shield}$ is a crucial bottleneck in previous studies of the LW radiation required for direct collapse [60,102,113,114] since in the case where the LW flux is anisotropic and sourced exterior to the cloud, the success of direct collapse to SMBHs crucially depends on the ability of the radiation to penetrate the outer shell of molecular hydrogen to reach the core region. Our scenario is different: the baryon cloud is immersed in the nearly homogeneous and isotropic background of LW photons from the relic particle decay, and the core region with the highest DM density experiences the strongest radiation intensity. Therefore, the LW radiation can reach the H_2 molecules in the core region even in the optically thick regime. Since the radiation no longer needs to penetrate through the cloud, the shield fraction is greatly reduced. Furthermore, as the shielding is reduced, the LW photons can dissociate H_2 more effectively, further decreasing the shielding. In addition, since the DM halo is larger than the

baryonic cloud, the exterior region of the baryonic cloud is irradiated by the exterior portion of the halo as well as *in situ* photons. Even if the DM is less dense in this region, the significant exterior flux makes it unlikely that the cloud could fragment in the exterior regions but not the interior, as was suggested in Ref. [46].

To quantify the uncertainty in the shielding, we introduce a new parameter $\varepsilon_{\rm sh}$ to track how much radiation is being shielded. We parametrize the *in situ* shield fraction by

$$f_{in\ situ} = 1 - \varepsilon_{\rm sh}(1 - f_{\rm shield}), \tag{13}$$

so that $\varepsilon_{\rm sh} = 1$ corresponds to full self-shielding and $\varepsilon_{\rm sh} = 0$ corresponds to no shielding. We present our results for several values of this shielding parameter, although we expect that it should be very close to 0.

Particle decay constraints—For both these mechanisms, we must tune the mass of the decaying particle so that they produce LW photons. In addition, the fraction of decaying dark matter must satisfy observational constraints [99–101] which require no more than $\sim 1\%$ of dark matter to decay in the early universe, although as we will see the decay fractions we require here for a successful collapse fall easily shy of this mark.

A natural candidate for decaying DM in the LW mass range are ALPs [87–97,115,116] since they are well-motivated dark matter candidates which naturally decay to two photons. In this scenario, we must restrict the mass to range from 22.4 to 27.2 eV. Although this region cannot contain the QCD axion [115,116], the parameter space is still available for the more generic ALPs, with the strongest constraints from cosmic optical background (COB) observations [80,81].
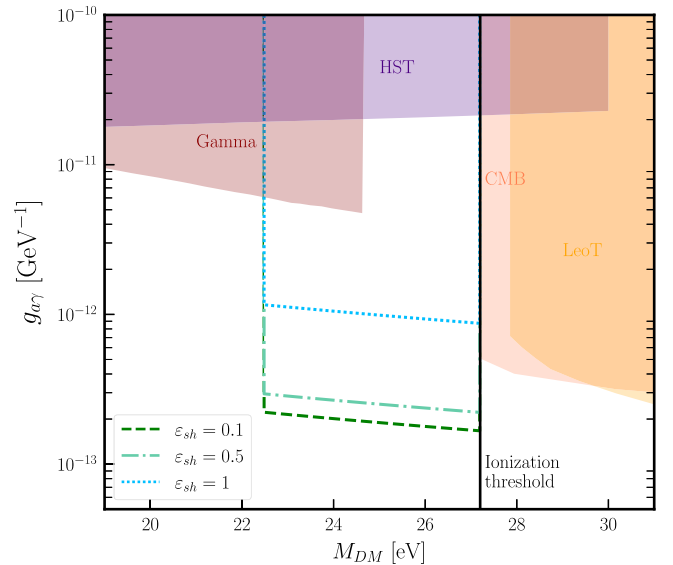

FIG. 1. ALP parameter space and relevant constraints [80–86,115–117] for successful direct collapse at $z \sim 20$. We demonstrate the results for three choices of $\varepsilon_{\rm sh}$.
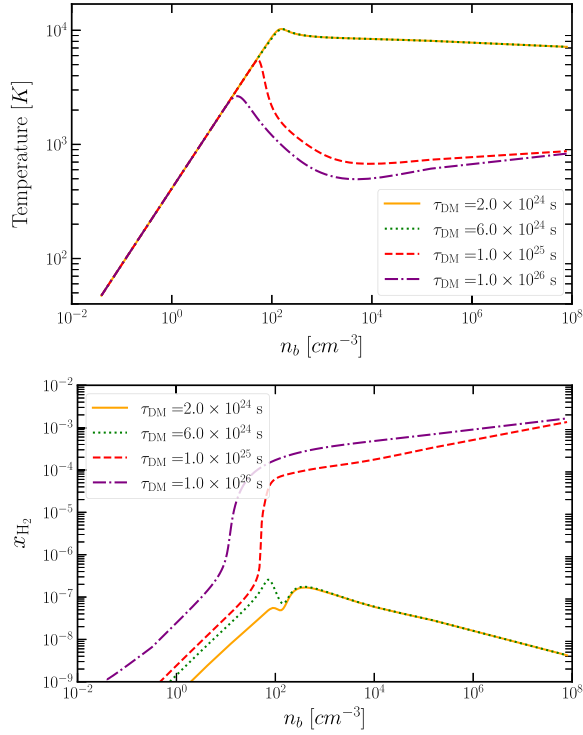
FIG. 2. Temperature and H_2 fraction during the collapse in the case of DM undergoing two-body decay. We see a clear bifurcation behavior here: if the DM lifetime is below a threshold value $\sim 6 \times 10^{24}$ s, the formation of H_2 is inhibited and, consequently, the temperature stays at 10^4 K during collapse. The DM mass is chosen to be 25 eV and the halo collapses at $z \sim 20$.

FIG. 3. Energy fractions of particle decay required to trigger direct collapse in the case of early decaying X and DM, where the three curves on each plot are for different amounts of shielding. We show the parameter space for three-body decay (left panels) and two-body decay (right panels). The DM lifetime is chosen to be 2×10^{24} s and X is set to decay at $z = 22$. The only relevant constraint is from the CMB anisotropy for X decay [84], which is plotted on the bottom left panel. The halo is set to collapse at $z \sim 20$ here.

The parameter space in the conventional axion-photon coupling $g_{a\gamma}$ and dark matter mass M_{DM} is shown in Fig. 1, where the minimum decay rates for the successful collapse are shown for different shielding assumptions and will be discussed in more detail in the following section. We include the constraints from the Hubble Space Telescope (HST) observation of cosmic optical background (COB) anisotropy [80,81] and gamma-ray attenuation [82,83,86]. In addition, if the ALP mass exceeds the hydrogen ionization threshold, it is strongly constrained by CMB anisotropies [84,117] and the heating of the dwarf galaxy Leo T [85]. Notably, in Ref. [84], the constraint is derived assuming a photon injection spectrum with a narrow but finite width, leading to constraints that saturate below the ionization threshold at 27.2 eV. This assumption is not valid in the case of ALP decay, so we cut off this constraint at the ionization threshold. We emphasize that the available parameter space for $\varepsilon_{sh} = 1$ is not eliminated even if we use the CMB anisotropy constraint without the cutoff.

For the more generic short-lived particle, a well-motivated scenario is the *string axiverse* [95], in which there are naturally many BSM particles over a wide range of masses. Just one of these particles would need to have the appropriate mass to accommodate our proposed mechanism. In this scenario, the relevant constraints are those
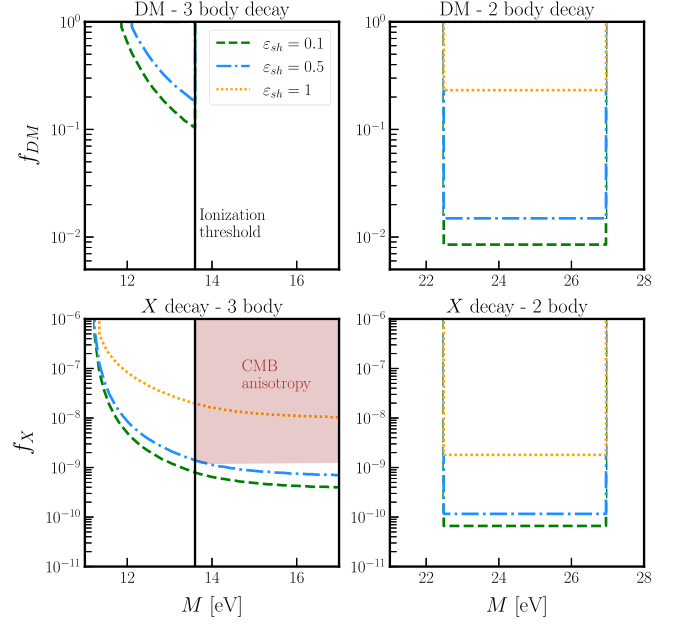
which constrain the maximum evaporating fraction of dark matter [84,99–101].

Results and discussion—An example of the temperature and chemical evolution during the collapse is shown in Fig. 2, where one can understand the forward progress of time as moving to the right on the curves. We observe a bifurcation behavior between the successful and failed collapse process: a successful direct collapse is characterized by a final temperature near 10^4 K with H_2 fraction $\ll 10^{-5}$. These criteria are used to check the collapse outcome in our parameter space search.

In the case of the X particle decaying early (around $z \sim 20$ here), only a small fraction of the total DM density is required to allow direct-collapse SMBH formation. We show the viability of this scenario, together with the DM decay, in Fig. 3. As seen from the top left panel of Fig. 3, if self shielding is not reduced, DM with three-body decay cannot produce enough LW radiation for direct collapse. This is consistent with the critical curve results obtained in Ref. [46]. For photons below the hydrogen ionization threshold, the fraction f_X (at a time long before the epoch of decay) is constrained to be $\lesssim 10^{-2}$ from CMB spectral distortion observed by COBE/FIRAS. Above the threshold, however, the injection is subject to strong constraints from CMB anisotropies, and we include this constraint on the
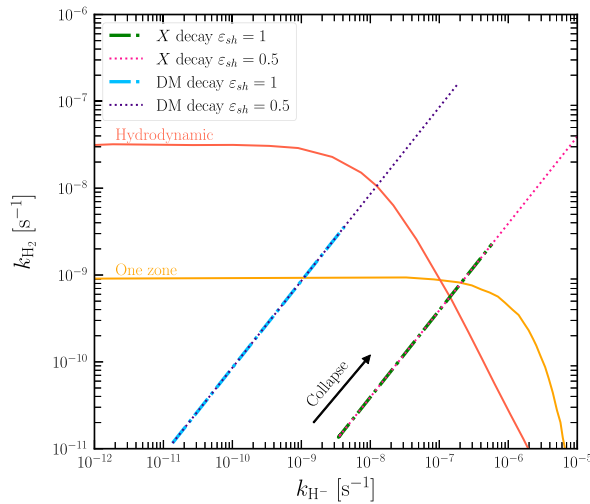
FIG. 4. Comparison of the critical curves with the reaction rates (in a successful direct collapse) calculated in our dynamical one-zone approach. The critical curves are taken from Ref. [102] (one-zone model) and Ref. [114] (hydrodynamic simulation). Both critical curves take $\lambda_{\text{Jeans}}/4$ as the characteristic length for computing the H_2 column density. For a moderate reduction of the shield fraction, the final rates go beyond the critical values required even in hydrodynamic simulations. The rates are calculated for an early decayed particle (three-body decay) with mass 13 eV and $f_X = 10^{-7}$ that decays at $z = 25$, and for DM (two-body decay) with mass 25 eV and lifetime 2×10^{24} s.

bottom left panel for a particle with lifetime 10^{14} s. For comparison, we are interested in lifetimes around 10^{15} s, reducing the plotted constraints. We do not need to tune the particle lifetime to exactly coincide with the collapse time. For a halo to collapse at $z = 20$, viable choices for the X lifetime span a wide range from $z \sim 50$ to $z \sim 4$, because decay is a stochastic process.

When the LW radiation is constant, it is convenient to derive the critical dissociation and detachment rates required as a simple check for successful direct collapse. Such requirement, plotted on the $k_{H_2} - k_{H^-}$ plane, forms the so called critical curve [102,103,114]. However, a direct comparison between our results and the critical curve is not straightforward. Firstly, the LW produced by particle decay is no longer a single point on the $k_{H_2} - k_{H^-}$ plane, with lower reaction rates (due to lower specific intensity) at the beginning of the collapse but increasing significantly at later stage. Another obstruction comes from the fact that all previous critical curve results [102,103,114] assumed an external source of LW radiation with full self-shielding ($\varepsilon_{\text{sh}} = 1$). In our case, the shield fraction is expected to be heavily reduced due to the *in situ* emission of LW photons. Nevertheless, we present the critical curves in Fig. 4 as a useful check. Naively, it would seem that the LW radiation cannot reach the critical value required from hydrodynamic simulations when $\varepsilon_{\text{sh}} = 1$, but even a moderate reduction of the shield fraction can increase the final rates by several

orders of magnitude, exceeding the threshold required for successful collapse.

Conclusion—We have shown that the decay of DM or a short-lived particle X can effectively halt the production of molecular hydrogen, allowing direct collapse to a SMBH to occur. While previous studies found that particle decay may not lead to collapse, we found that dynamically including the adiabatic contraction of the DM halo, as well as considering lower shielding than in the case where the LW background comes from an exterior source, allowed our model to be successful. To go beyond the one-zone approach that we adopt in this work, a full-scale simulation that takes into account a realistic halo profile and *in situ* effects—similar to the one in Ref. [118]—is needed to confirm our result.

The decay of ALPs in our mass range of interest can produce light in the optical and UV range. Interestingly, as pointed out in Ref. [119], such decay could explain the COB excess observed by New Horizons' Long Range Reconnaisance Imager (LORRI) [120]. Later studies, however, concluded that ALP decay is unlikely to produce such an excess due to the COB anisotropy at 606 nm and gamma ray attenuation [80,81,86,121]. Probing these so called "blue axions" offers an opportunity to test our proposed mechanism. With future HST measurements at higher frequencies, a large portion of our parameter space could be explored [81]. It would be of great interest if the mystery of high redshift SMBHs and the question of DM can be answered simultaneously.

[1] K. Inayoshi, E. Visbal, and Z. Haiman, The assembly of the first massive black holes, Annu. Rev. Astron. Astrophys. **58**, 27 (2020).

[2] L. Mayer and S. Bonoli, The route to massive black hole formation via merger-driven direct collapse: A review, Rep. Prog. Phys. **82**, 016901 (2018).

[3] M. Volonteri, Formation of supermassive black holes, Astron. Astrophys. Rev. **18**, 279 (2010).

[4] T. Wiklind, B. Mobasher, and V. Bromm, *The First Galaxies: Theoretical Predictions and Observational Clues* (Springer Science & Business Media, New York, 2012), Vol. 396.

[5] A. Bogdan *et al.*, Evidence for heavy seed origin of early supermassive black holes from a z~10 X-ray quasar, Nat. Astron. **8**, 126 (2024).

[6] S. Sethi, Z. Haiman, and K. Pandey, Supermassive black hole formation at high redshifts through a primordial magnetic field, Astrophys. J. 721, 615 (2010).

[7] J. P. Gardner *et al.*, The James Webb Space Telescope, Space Sci. Rev. 123, 485 (2006).

[8] H. Übler, R. Maiolino, E. Curtis-Lake, P. G. Pérez-González, M. Curti, M. Perna *et al.*, GA-NIFS: A massive black hole in a low-metallicity AGN at z ∼ 5.55 revealed by JWST/NIRSpec IFS, Astron. Astrohys. 677, A145 (2023).

[9] R. L. Larson, S. L. Finkelstein, D. D. Kocevski, T. A. Hutchison, J. R. Trump, P. Arrabal Haro *et al.*, A CEERS discovery of an accreting supermassive black hole 570 Myr after the big bang: Identifying a progenitor of massive z > 6 quasars, Astrophys. J. Lett. 953, L29 (2023).

[10] Y. Harikane, Y. Zhang, K. Nakajima, M. Ouchi, Y. Isobe, Y. Ono, Shun Hatano, Yi Xu, and H. Umeda, A JWST/NIRSpec first census of broad-line AGNs at z = 1–7: Detection of 10 faint AGNs with M_{BH} 10^6–$10^8 M_\odot$ and their host galaxy properties, Astrophys. J. 959, 39 (2023).

[11] A. C. Carnall, R. J. McLure, J. S. Dunlop, D. J. McLeod, V. Wild, F. Cullen *et al.*, A massive quiescent galaxy at redshift 4.658, Nature (London) 619, 716 (2023).

[12] M. Onoue, K. Inayoshi, X. Ding, W. Li, Z. Li, J. Molina, A. K. Inoue, L. Jiang, and L. C. Ho, A candidate for the least-massive black hole in the first 1.1 billion years of the universe, Astrophys. J. Lett. 942, L17 (2023).

[13] D. D. Kocevski, M. Onoue, K. Inayoshi, J. R. Trump, P. Arrabal Haro, A. Grazian *et al.*, Hidden little monsters: Spectroscopic identification of low-mass, broad-line AGNs at z > 5 with CEERS, Astrophys. J. Lett. 954, L4 (2023).

[14] X. Fan, E. Bañados, and R. A. Simcoe, Quasars and the intergalactic medium at cosmic dawn, Annu. Rev. Astron. Astrophys. 61, 373 (2023).

[15] R. Maiolino *et al.*, A small and vigorous black hole in the early Universe, Nature (London) 627, 59 (2024).

[16] N. Banik, J. C. Tan, and P. Monaco, The formation of supermassive black holes from Population III.1 seeds. I. Cosmic formation histories and clustering properties, Mon. Not. R. Astron. Soc. 483, 3592 (2019).

[17] T. Ohkubo, K. Nomoto, H. Umeda, N. Yoshida, and S. Tsuruta, Evolution of very massive Population III stars with mass accretion from pre-main sequence to collapse, Astrophys. J. 706, 1184 (2009).

[18] P. Kroupa, L. Subr, T. Jerabkova, and L. Wang, Very high redshift quasars and the rapid emergence of supermassive black holes, Mon. Not. R. Astron. Soc. 498, 5652 (2020).

[19] S. Balberg and S. L. Shapiro, Gravothermal collapse of self-interacting dark matter halos and the origin of massive black holes, Phys. Rev. Lett. 88, 101301 (2002).

[20] J. Pollack, D. N. Spergel, and P. J. Steinhardt, Supermassive black holes from ultra-strongly self-interacting dark matter, Astrophys. J. 804, 131 (2015).

[21] J. Koda and P. R. Shapiro, Gravothermal collapse of isolated self-interacting dark matter haloes: N-body simulation versus the fluid model, Mon. Not. R. Astron. Soc. 415, 1125 (2011).

[22] W.-X. Feng, H.-B. Yu, and Y.-M. Zhong, Seeding supermassive black holes with self-interacting dark matter: A unified scenario with baryons, Astrophys. J. Lett. 914, L26 (2021).

[23] H. Xiao, X. Shen, P. F. Hopkins, and K. M. Zurek, SMBH seeds from dissipative dark matter, J. Cosmol. Astropart. Phys. 07 (2021) 039.

[24] Y. B. Zel'dovich and I. D. Novikov, The hypothesis of cores retarded during expansion and the hot cosmological model, Sov. Astron. 10, 602 (1966).

[25] S. Hawking, Gravitationally collapsed objects of very low mass, Mon. Not. R. Astron. Soc. 152, 75 (1971).

[26] B. J. Carr and S. Hawking, Black holes in the early Universe, Mon. Not. R. Astron. Soc. 168, 399 (1974).

[27] G. F. Chapline, Cosmological effects of primordial black holes, Nature (London) 253, 251 (1975).

[28] B. Carr, K. Kohri, Y. Sendouda, and J. Yokoyama, Constraints on primordial black holes, Rep. Prog. Phys. 84, 116902 (2021).

[29] R. Bean and J. Magueijo, Could supermassive black holes be quintessential primordial black holes?, Phys. Rev. D 66, 063505 (2002).

[30] N. Duchting, Supermassive black holes from primordial black hole seeds, Phys. Rev. D 70, 064015 (2004).

[31] M. Y. Khlopov, S. G. Rubin, and A. S. Sakharov, Primordial structure of massive black hole clusters, Astropart. Phys. 23, 265 (2005).

[32] V. Dokuchaev, Y. Eroshenko, and S. Rubin, Quasars formation around clusters of primordial black holes, Gravitation Cosmol. 11, 99 (2005).

[33] M. Kawasaki, A. Kusenko, and T. T. Yanagida, Primordial seeds of supermassive black holes, Phys. Lett. B 711, 1 (2012).

[34] B. Carr, S. Clesse, J. Garcia-Bellido, M. Hawkins, and F. Kuhnel, Observational evidence for primordial black holes: A positivist perspective, Phys. Rep. 1054, 1 (2024).

[35] M. M. Flores and A. Kusenko, Primordial black holes from long-range scalar forces and scalar radiative cooling, Phys. Rev. Lett. 126, 041101 (2021).

[36] M. M. Flores and A. Kusenko, Primordial black holes as a dark matter candidate in theories with supersymmetry and inflation, J. Cosmol. Astropart. Phys. 05 (2023) 013.

[37] M. M. Flores, Y. Lu, and A. Kusenko, Structure formation after reheating: Supermassive primordial black holes and Fermi ball dark matter, Phys. Rev. D 108, 123511 (2023).

[38] V. Bromm and A. Loeb, Formation of the first supermassive black holes, Astrophys. J. 596, 34 (2003).

[39] J.-H. Choi, I. Shlosman, and M. C. Begelman, Supermassive black hole formation at high redshifts via direct collapse: Physical processes in the early stage, Astrophys. J. 774, 149 (2013).

[40] C. Shang, G. L. Bryan, and Z. Haiman, Supermassive black hole formation by direct collapse: Keeping protogalactic gas H_2 free in dark matter haloes with virial temperatures $T_{vir} \gtrsim 10^4$ K, Mon. Not. R. Astron. Soc. 402, 1249 (2010).

[41] P. L. Biermann and A. Kusenko, Relic keV sterile neutrinos and reionization, Phys. Rev. Lett. 96, 091301 (2006).

[42] J. Stasielak, P. L. Biermann, and A. Kusenko, Thermal evolution of the primordial clouds in warm dark matter models with keV sterile neutrinos, Astrophys. J. 654, 290 (2007).

[43] D. Spolyar, K. Freese, and P. Gondolo, Dark matter and the first stars: A new phase of stellar evolution, Phys. Rev. Lett. 100, 051101 (2008).

[44] A. Natarajan, J. C. Tan, and B. W. O'Shea, Dark matter annihilation and primordial star formation, Astrophys. J. 692, 574 (2009).

[45] I. J. Araya and N. D. Padilla, Dark matter annihilation energy output and its effects on the high-z IGM, Mon. Not. R. Astron. Soc. 445, 850 (2014).

[46] A. Friedlander, S. Schon, and A. C. Vincent, Supermassive black hole seeds from sub-keV dark matter, J. Cosmol. Astropart. Phys. 06 (2023) 033.

[47] M. Dijkstra, Z. Haiman, A. Mesinger, and J. S. B. Wyithe, Fluctuations in the high-redshift Lyman-Werner background: Close halo pairs as the origin of supermassive black holes, Mon. Not. R. Astron. Soc. 391, 1961 (2008).

[48] Y. Lu, Z. S. C. Picker, and A. Kusenko, Feeding plankton to whales: High-redshift supermassive black holes from tiny black hole explosions, Phys. Rev. D 109, 123016 (2024).

[49] S. Lepp and J. M. Shull The kinetic theory of H2 dissociation, Astrophys. J. 270, 578 (1983).

[50] D. Hollenbach and C. F. McKee, Molecule formation and infrared emission in fast interstellar shocks. I physical processes, Astrophys. J. Suppl. Ser. 41, 555 (1979).

[51] S. P. Oh and Z. Haiman, Second-generation objects in the universe: Radiative cooling and collapse of halos with virial temperatures above 10^4 kelvin, Astrophys. J. 569, 558 (2002).

[52] K. Omukai, R. Schneider, and Z. Haiman, Can supermassive black holes form in metal-enriched high-redshift protogalaxies?, Astrophys. J. 686, 801 (2008).

[53] K. Omukai, Primordial star formation under far-ultraviolet radiation, Astrophys. J. 546, 635 (2001).

[54] F. Becerra, F. Marinacci, V. Bromm, and L. E. Hernquist, Assembly of supermassive black hole seeds, Mon. Not. R. Astron. Soc. 480, 5029 (2018).

[55] J. Jeon, V. Bromm, B. Liu, and S. L. Finkelstein, Physical pathways for JWST-observed supermassive black holes in the early universe, arXiv:2402.18773.

[56] Z. Haiman, M. J. Rees, and A. Loeb, Destruction of molecular hydrogen during cosmological reionization, Astrophys. J. 476, 458 (1997).

[57] B. Cyr, H. Jiao, and R. Brandenberger, Massive black holes at high redshifts from superconducting cosmic strings, Mon. Not. R. Astron. Soc. 517, 2221 (2022).

[58] B. Agarwal, S. Khochfar, J. L. Johnson, E. Neistein, C. Dalla Vecchia, and M. Livio, Ubiquitous seeding of supermassive black holes by direct collapse, Mon. Not. R. Astron. Soc. 425, 2854 (2012).

[59] M. Dijkstra, A. Ferrara, and A. Mesinger, Feedback-regulated supermassive black hole seed formation, Mon. Not. R. Astron. Soc. 442, 2036 (2014).

[60] C. Shang, G. Bryan, and Z. Haiman, Supermassive black hole formation by direct collapse: Keeping protogalactic gas H_2–free in dark matter halos with virial temperatures T_vir >~ 10^4 K, Mon. Not. R. Astron. Soc. 402, 1249 (2010).

[61] T. Hartwig, S. C. O. Glover, R. S. Klessen, M. A. Latif, and M. Volonteri, How an improved implementation of H2 self-shielding influences the formation of massive stars and black holes, Mon. Not. R. Astron. Soc. 452, 1233 (2015).

[62] K. Inayoshi and T. L. Tanaka, The suppression of direct collapse black hole formation by soft X-ray irradiation, Mon. Not. R. Astron. Soc. 450, 4350 (2015).

[63] M. A. Latif, S. Bovino, C. Van Borm, T. Grassi, D. R. G. Schleicher, and M. Spaans, A UV flux constraint on the formation of direct collapse black holes, Mon. Not. R. Astron. Soc. 443, 1979 (2014).

[64] M. C. Begelman, M. Volonteri, and M. J. Rees, Formation of supermassive black holes by direct collapse in pregalactic halos, Mon. Not. R. Astron. Soc. 370, 289 (2006).

[65] L. Haemmerlé, General-relativistic instability in rapidly accreting supermassive stars: The impact of rotation, Astron. Astrophys. 650, A204 (2021).

[66] M. A. Latif, D. R. G. Schleicher, W. Schmidt, and J. Niemeyer, Black hole formation in the early universe, Mon. Not. R. Astron. Soc. 433, 1607 (2013).

[67] J.-H. Choi, I. Shlosman, and M. C. Begelman, Supermassive black hole formation at high redshifts via direct collapse in a cosmological context, Mon. Not. R. Astron. Soc. 450, 4411 (2015).

[68] M. C. Begelman and I. Shlosman, Angular momentum transfer and lack of fragmentation in self-gravitating accretion flows, Astrophys. J. Lett. 702, L5 (2009).

[69] I. Shlosman, J. Frank, and M. C. Begelman, Bars within bars—A mechanism for fuelling active galactic nuclei, Nature (London) 338, 45 (1989).

[70] I. Shlosman, M. C. Begelman, and J. Frank, The fuelling of active galactic nuclei, Nature (London) 345, 679 (1990).

[71] D. J. Eisenstein and A. Loeb, Origin of quasar progenitors from the collapse of low spin cosmological perturbations, Astrophys. J. 443, 11 (1995).

[72] S. M. Koushiappas, J. S. Bullock, and A. Dekel, Massive black hole seeds from low angular momentum material, Mon. Not. R. Astron. Soc. 354, 292 (2004).

[73] K. Inayoshi, K. Omukai, and E. J. Tasker, Formation of an embryonic supermassive star in the first galaxy, Mon. Not. R. Astron. Soc. 445, L109 (2014).

[74] C. Van Borm, S. Bovino, M. A. Latif, D. R. G. Schleicher, M. Spaans, and T. Grassi, Effects of turbulence and rotation on protostar formation as a precursor of massive black holes, Astron. Astrophys. 572, A22 (2014).

[75] F. Becerra, T. H. Greif, V. Springel, and L. Hernquist, Formation of massive protostars in atomic cooling haloes, Mon. Not. R. Astron. Soc. 446, 2380 (2015).

[76] J. A. Regan, P. H. Johansson, and M. G. Haehnelt, Numerical resolution effects on simulations of massive black hole seeds, Mon. Not. R. Astron. Soc. 439, 1160 (2014).

[77] S. Chandrasekhar, The dynamical instability of gaseous masses approaching the Schwarzschild limit in general relativity, Astrophys. J. 140, 417 (1964).

[78] Y. B. Zel'dovich and I. D. Novikov, Stars and Relativity (Dover Publications, Mineola, New York, 2014).

[79] S. L. Shapiro and S. A. Teukolsky, Black Holes, White Dwarfs, and Neutron Stars: The Physics of Compact Objects (Wiley-Vch Verlag, Berlin, 1983), 10.1002/9783527617661.

[80] K. Nakayama and W. Yin, Anisotropic cosmic optical background bound for decaying dark matter in light of the LORRI anomaly, Phys. Rev. D **106**, 103505 (2022).

[81] P. Carenza, G. Lucente, and E. Vitagliano, Probing the blue axion with cosmic optical background anisotropies, Phys. Rev. D **107**, 083032 (2023).

[82] A. Korochkin, A. Neronov, and D. Semikoz, Search for spectral features in extragalactic background light with gamma-ray telescopes, Astron. Astrophys. **633**, A74 (2020).

[83] A. Korochkin, A. Neronov, and D. Semikoz, Search for decaying eV-mass axion-like particles using gamma-ray signal from blazars, J. Cosmol. Astropart. Phys. 03 (2020) 064.

[84] B. Bolliet, J. Chluba, and R. Battye, Spectral distortion constraints on photon injection from low-mass decaying particles, Mon. Not. R. Astron. Soc. **507**, 3148 (2021).

[85] D. Wadekar and Z. Wang, Strong constraints on decay and annihilation of dark matter from heating of gas-rich dwarf galaxies, Phys. Rev. D **106**, 075007 (2022).

[86] J. L. Bernal, A. Caputo, G. Sato-Polito, J. Mirocha, and M. Kamionkowski, Seeking dark matter with γ-ray attenuation, Phys. Rev. D **107**, 103046 (2023).

[87] R. D. Peccei and H. R. Quinn, *CP* conservation in the presence of instantons, Phys. Rev. Lett. **38**, 1440 (1977).

[88] S. Weinberg, A new light boson?, Phys. Rev. Lett. **40**, 223 (1978).

[89] F. Wilczek, Problem of strong *P* and *T* invariance in the presence of instantons, Phys. Rev. Lett. **40**, 279 (1978).

[90] J. E. Kim, Weak interaction singlet and strong *CP* invariance, Phys. Rev. Lett. **43**, 103 (1979).

[91] M. A. Shifman, A. I. Vainshtein, and V. I. Zakharov, Can confinement ensure natural *CP* invariance of strong interactions?, Nucl. Phys. **B166**, 493 (1980).

[92] M. Dine, W. Fischler, and M. Srednicki, A simple solution to the strong *CP* problem with a harmless axion, Phys. Lett. **104B**, 199 (1981).

[93] A. R. Zhitnitsky, On possible suppression of the axion hadron interactions. (In Russian), Sov. J. Nucl. Phys. **31**, 260 (1980).

[94] P. Svrcek and E. Witten, Axions in string theory, J. High Energy Phys. 06 (2006) 051.

[95] A. Arvanitaki, S. Dimopoulos, S. Dubovsky, N. Kaloper, and J. March-Russell, String axiverse, Phys. Rev. D **81**, 123530 (2010).

[96] B. S. Acharya, K. Bobkov, and P. Kumar, An M theory solution to the strong *CP* problem and constraints on the axiverse, J. High Energy Phys. 11 (2010) 105.

[97] M. Dine, G. Festuccia, J. Kehayias, and W. Wu, Axions in the landscape and string theory, J. High Energy Phys. 01 (2011) 012.

[98] C. O'Hare, cajohare/axionlimits: Axionlimits, https://cajohare.github.io/AxionLimits/, 2020.

[99] V. Poulin, P. D. Serpico, and J. Lesgourgues, A fresh look at linear cosmological constraints on a decaying dark matter component, J. Cosmol. Astropart. Phys. 08 (2016) 036.

[100] L. Xiao, L. Zhang, R. An, C. Feng, and B. Wang, Fractional dark matter decay: Cosmological imprints and observational constraints, J. Cosmol. Astropart. Phys. 01 (2020) 045.

[101] S. Alvi, T. Brinckmann, M. Gerbino, M. Lattanzi, and L. Pagano, Do you smell something decaying? Updated linear constraints on decaying dark matter scenarios, J. Cosmol. Astropart. Phys. 11 (2022) 015.

[102] J. Wolcott-Green, Z. Haiman, and G. L. Bryan, Beyond Jcrit: A critical curve for suppression of H2-cooling in protogalaxies, Mon. Not. R. Astron. Soc. **469**, 3329 (2017).

[103] B. Agarwal, B. Smith, S. Glover, P. Natarajan, and S. Khochfar, New constraints on direct collapse black hole formation in the early universe, Mon. Not. R. Astron. Soc. **459**, 4209 (2016).

[104] P. R. Shapiro and H. Kang, Hydrogen molecules and the radiative cooling of pregalactic shocks, Astrophys. J. **318**, 32 (1987).

[105] G. Steigman, C. L. Sarazin, H. Quintana, and J. Faulkner, Dynamical interactions and astrophysical effects of stable heavy neutrinos, Astron. J. **83**, 1050 (1978).

[106] Y. B. Zeldovich, A. A. Klypin, M. Y. Khlopov, and V. M. Chechetkin, Astrophysical constraints on the mass of heavy stable neutral leptons, Sov. J. Nucl. Phys. **31**, 664 (1980).

[107] B. S. Ryden and J. E. Gunn, Galaxy formation by gravitational collapse, Astrophys. J. **318**, 15 (1987).

[108] S. Faber, Contraction of dark matter galactic halos due to baryonic infall, Astrophys. J. **301**, 27 (1986).

[109] O. J. Eggen, D. Lynden-Bell, and A. R. Sandage, Evidence from the motions of old stars that the galaxy collapsed., Astrophys. J. **136**, 748 (1962).

[110] K. Freese, T. Rindler-Daller, D. Spolyar, and M. Valluri, Dark stars: A review, Rep. Prog. Phys. **79**, 066902 (2016).

[111] D. C. Morton and H. L. Dinerstein, Interstellar molecular hydrogen toward zeta puppis, Astrophys. J. **204**, 1 (1976).

[112] B. T. Draine and F. Bertoldi, Structure of stationary photodissociation fronts, Astrophys. J. **468**, 269 (1996).

[113] J. Wolcott-Green, Z. Haiman, and G. L. Bryan, Photodissociation of H2 in protogalaxies: Modelling self-shielding in three-dimensional simulations, Mon. Not. R. Astron. Soc. **418**, 838 (2011).

[114] Y. Luo, I. Shlosman, K. Nagamine, and T. Fang, Direct collapse to supermassive black hole seeds: The critical conditions for suppression of H2 cooling, Mon. Not. R. Astron. Soc. **492**, 4917 (2020).

[115] C. O'Hare, cajohare/AxionLimits: AxionLimits, 2020, 10.5281/zenodo.3932430.

[116] C. A. J. O'Hare, Cosmology of axion dark matter, Proc. Sci. COSMICWISPers (2024) 040.

[117] S. K. Acharya, B. Cyr, and J. Chluba, Constraining broad photon spectrum injections from exotic and astrophysical sources, arXiv:2309.00975.

[118] A. Stacy, A. H. Pawlik, V. Bromm, and A. Loeb, The mutual interaction between Population III stars and self-annihilating dark matter, Mon. Not. R. Astron. Soc. **441**, 822 (2014).

[119] J. L. Bernal, G. Sato-Polito, and M. Kamionkowski, Cosmic optical background excess, dark matter, and line-intensity mapping, Phys. Rev. Lett. **129**, 231301 (2022).

[120] T. R. Lauer *et al.*, Anomalous flux in the cosmic optical background detected with new horizons observations, Astrophys. J. Lett. **927**, L8 (2022).

[121] H. Wang *et al.*, A spectroscopic search for optical emission lines from dark matter decay, arXiv:2311.05476.

[122] C. R. Harris, K. J. Millman, S. J. van der Walt, R. Gommers, P. Virtanen, D. Cournapeau *et al.*, Array programming with NumPy, Nature (London) **585**, 357 (2020).

[123] P. Virtanen, R. Gommers, T. E. Oliphant, M. Haberland, T. Reddy, D. Cournapeau *et al.*, SciPy1.0: Fundamental algorithms for scientific computing in PYTHON, Nat. Methods **17**, 261 (2020).

[124] J. D. Hunter, MATPLOTLIB: A 2d graphics environment, Comput. Sci. Eng. **9**, 90 (2007).